#### **ORIGINAL ARTICLE**



# Diagnosis of treatment-related changes in children and adolescents with brain and spinal tumors: a cost-effectiveness analysis using MRI and [18 F]FET PET

Jurij Rosen<sup>1</sup> · Jan-Michael Werner<sup>2</sup> · Garry S. Ceccon<sup>2</sup> · Elena K. Rosen<sup>2</sup> · Michael M. Wollring<sup>2,3</sup> · Isabelle Stetter<sup>2</sup> · Philipp Lohmann<sup>3,4</sup> · Felix M. Mottaghy<sup>4,5,6</sup> · Lisbeth Marner<sup>7,8</sup> · Ian Law<sup>7</sup> · Gereon R. Fink<sup>2,3</sup> · Karl-Josef Langen<sup>3,4,6</sup> · Norbert Galldiks<sup>2,3,6</sup>

Received: 20 February 2025 / Accepted: 20 May 2025 / Published online: 4 June 2025 © The Author(s) 2025

#### **Abstract**

**Purpose** PET using the radiolabeled amino acid O- $(2-[^{18}F]$ -fluoroethyl)-L-tyrosine ([ $^{18}F$ ]FET) has considerable clinical value for follow-up evaluation of central nervous system tumors in children and adolescents. As medical procedures must be justified socio-economically, we determined cost-effectiveness of [ $^{18}F$ ]FET PET for identification of treatment-related changes.

**Methods** We analyzed clinical data from two different studies that assessed the value of FET PET to differentiate between brain and spinal tumor relapse and treatment-related changes in children and adolescents. Cost calculation was based on the German statutory health insurance system perspective. Due to subtle differences in the diagnostic approach of the studies, two separate clinical scenarios including 80 patients with 105 lesions were considered: Decision tree model 1 determined cost-effectiveness of simultaneous [<sup>18</sup>F]FET PET and MRI in comparison to MRI alone to identify treatment-related changes. Decision tree model 2 determined cost-effectiveness of [<sup>18</sup>F]FET PET alone to identify treatment-related changes when routine MRI findings were suspicious for tumor relapse. Deterministic and probabilistic sensitivity analyses tested the robustness of the results.

Results Model 1 revealed that the rate of identified treatment-related changes increased by 52% when adding [<sup>18</sup>F]FET PET to MRI, resulting in costs of €3,314.51 for each additional correctly identified lesion with treatment-related changes by [<sup>18</sup>F] FET PET that MRI would have misclassified. Model 2 revealed that [<sup>18</sup>F]FET PET correctly identified treatment-related changes in 90% of lesions when routine MRI findings were suspicious for tumor relapse, resulting in costs of €1,740.37 for each lesion.

**Conclusion** Integrating [<sup>18</sup>F]FET PET in the follow-up of in children and adolescents with brain and spinal tumor may help improving patient care at acceptable costs.

**Keywords** Amino acid PET · Economic evaluation · Treatment monitoring · Tumor relapse

- Norbert Galldiks n.galldiks@fz-juelich.de; norbert.galldiks@uk-koeln.de
- Department of Psychiatry, Faculty of Medicine and University Hospital Cologne, University of Cologne, Cologne, Germany
- Department of Neurology, Faculty of Medicine and University Hospital Cologne, University of Cologne, Kerpener St. 62, 50937 Cologne, Germany
- Research Center Juelich, Institute of Neuroscience and Medicine (INM-3, INM-4), Leo-Brandt-St. 5, 52425 Juelich, Germany

- Department of Nuclear Medicine, RWTH University Hospital Aachen, Aachen, Germany
- Department of Radiology and Nuclear Medicine, Maastricht University Medical Center, Maastricht, The Netherlands
- <sup>6</sup> Center for Integrated Oncology Aachen Bonn Cologne Duesseldorf (CIO ABCD), Cologne, Germany
- Department of Clinical Physiology Nuclear Medicine and Nuclear Medicine, Copenhagen University Hospital Rigshospitalet, Copenhagen, Denmark
- Department of Clinical Physiology and Nuclear Medicine, Copenhagen University Hospital Bispebjerg, Copenhagen, Denmark



# Introduction

Pediatric central nervous system (CNS) tumors are the most frequent solid malignancy and the most common cause of cancer death in children [1, 2]. Given the heterogeneity of tumor entities with varying malignancy and location, management of CNS tumors in this group of patients to date remains challenging. Pediatric brain gliomas constitute the majority of CNS tumors, but advances in the management of adult brain tumors cannot directly be transferred to their pediatric counterparts as these show divergent molecular features, gene expression signatures and different clinical behavior [3, 4]. Regarding diagnostic imaging, contrast-enhanced anatomical MRI is the standard imaging procedure with excellent spatial resolution and high sensitivity for tumor detection at initial diagnosis and follow-up. However, the specificity of MR imaging to reliably differentiate between neoplastic and non-neoplastic lesions is limited. In particular, the differentiation of tumor relapse from treatment-related changes, in CNS tumors using contrastenhanced anatomical MRI alone remains challenging [5-11]. Notably, MRI signal changes such as an increase in the extent of contrast enhancement, newly occurring contrastenhancing lesions, or an increase of signal alterations on fluid-attenuated inversion recovery sequences may reflect either treatment-related changes or tumor relapse [5–11].

Considering the limited specificity of anatomical MRI for neoplastic tissue, amino acid PET has increasingly been used to metabolically assess cerebral lesions, primarily in adults [5, 12–18], but also in children and adolescents [19–25]. Although PET using 2-[18F]fluoro-2-deoxy-D-glucose ([18F]-FDG) is the tracer of choice for numerous diagnostic approaches in patients with cancer, the Response Assessment in Pediatric Neuro-Oncology (RAPNO) Working Group has recommended the use of PET with radiolabeled amino acids such as O-(2-[18F]fluoroethyl)-L-tyrosine ([18F]FET), as it provides a higher specificity for neoplastic tissue [2].

To date, several studies have addressed the value of [<sup>18</sup>F] FET PET in caring for children and adolescents with CNS tumors [19–25]. Among these, Marner et al. and Dunkl et al. [19, 23] investigated the diagnostic potential of [<sup>18</sup>F] FET PET for differentiating between tumor relapse and treatment-related changes at follow-up. Despite subtle differences in the diagnostic approach, both studies consistently showed that [<sup>18</sup>F]FET PET is of considerable value for diagnosing treatment-related changes [19, 23]. Notably, the authors concluded that static and dynamic [<sup>18</sup>F]FET PET parameters may add valuable diagnostic information that could not be provided by anatomical MRI alone.

Nevertheless, integrating [18F]FET PET in the care of children and adolescents with CNS tumors is associated

with additional costs that must be weighed against relevant clinical benefits for these patients, e.g., an improved diagnostic performance for the differentiation between tumor relapse and treatment-related changes. To our knowledge, no studies have yet addressed the cost-effectiveness of [18F] FET PET for monitoring CNS tumors in this age group. Several studies investigated the cost-effectiveness of [18F]FET PET imaging compared to MRI alone for increasing both the extent of resection [26] and the diagnostic yield following stereotactic biopsy [27], and for the response assessment to anticancer agents in adults with predominantly glioblastoma [28-30]. Besides, two other studies investigated the cost-effectiveness of [18F]FET PET for evaluating brain metastasis relapse following radiotherapy alone or multimodal therapy, including radiotherapy, targeted therapy, checkpoint inhibitors, and combinations thereof [31, 32]. These studies consistently suggested that [18F]FET PET use in adults is cost-effective for the clinical scenario examined. Nevertheless, these results are not directly transferable to children and adolescents as mechanisms of tumorigenesis, molecular genetic profiles, and clinical behavior of the neoplasms differ considerably between adult and pediatric patients [3, 4].

Considering the diagnostic improvements and additional costs of [<sup>18</sup>F]FET PET compared to anatomical MRI, the studies by Marner et al. [23] and Dunkl et al. [19] were evaluated regarding cost-effectiveness of [<sup>18</sup>F]FET PET to identify lesions consistent with treatment-related changes during follow-up. We performed this analysis from the perspective of the statutory health insurance system in Germany. To our knowledge, this is the first study investigating the cost-effectiveness of [<sup>18</sup>F]FET PET in children and adolescents suffering from CNS tumors.

# **Patients and methods**

# Input data

Input data were derived from the results of previously published studies by Marner et al. and Dunkl et al. that assessed the value of FET PET to differentiate between brain and spinal tumor relapse and treatment-related changes in children and adolescents [19, 23]. The institutional review board had approved these studies (Marner et al., file number: H-6–2014-095; Dunkl et al., file number: EK 022/14; clinical trial number: not applicable). Written informed consent for study participation and assessment of clinical data for scientific purposes had been obtained from the legal guardians of the minor study participants included in the study.

In the study by Marner et al., 97 children and adolescents (median age, 10 years; age range, 0.1–33 years) with 155



lesions (gliomas, 59%) were prospectively included for the evaluation of the added value of simultaneous [<sup>18</sup>F]FET PET and MRI compared to MRI alone [23]. In that study, inclusion criteria were suspicion or diagnosis of a primary CNS tumor before the age of 18 years, and scans were performed at initial diagnosis, before and after surgery, for response assessment, and at suspected relapse [23]. Twelve of these lesions were located at the spine. For the present analysis, only pretreated lesions were considered (i.e., radiotherapy, alkylating chemotherapy). Thus, the present analysis focuses on identifying lesions consistent with treatment-related changes in 64 patients with 83 lesions who underwent 92 FET PET and MRI scans (Supplemental Table 1).

In the study by Dunkl et al., 48 children and adolescents (median age at initial diagnosis, 13 years; age range, 1-18 years) with 69 [18F]FET PET scans performed at different stages of the disease were retrospectively identified. All patients had been referred consecutively because decision-making for further diagnostic procedures or treatment planning was difficult using the clinical presentation or MR imaging findings alone. Specifically, FET PET scans were performed for differential diagnosis of newly diagnosed cerebral lesions, for the differentiation between tumor relapse and treatment-related changes, assessment of response to chemotherapy, or the detection of residual tumor tissue after resection (Fig. 1) [19]. For the present study, 18 patients with 24 FET PET scans that served for the differentiation between tumor relapse and treatment-related changes when routine MRI were suspicious for tumor relapse were considered (Supplemental Table 2).

# Decision tree models for the assessment of the effectiveness

Similar to earlier studies [26–30], for each clinical scenario as described by Marner et al. and Dunkl et al., one separate decision tree model was developed to assess the effectiveness, i.e. diagnostic performance, of the combined FET PET and MRI approach compared with MRI alone (Model 1: Marner et al.), and of FET PET alone (Model 2: Dunkl et al.). The calculated effectiveness subsequently served as the

basis for the evaluation of cost-effectiveness, the primary outcome of the present study. Each model summarized the respective clinical scenario and neuroimaging, and assigned the examined lesions according to their respective imaging findings and, subsequently, their final diagnosis. These models were developed separately as subtle differences in the diagnostic approach of the studies warranted a distinct calculation of the effectiveness. Specifically, in model 1, FET PET and MRI were a priori conducted simultaneously, and their combined effectiveness compared to MRI alone to identify lesions consistent with treatment-related changes were compared. In model 2, a routine MRI had shown changes suspicious for tumor relapse, and prompted subsequent FET PET imaging.

Therefore, the effectiveness in model 1 was determined by comparing the effectiveness of combined FET PET and MRI with MRI alone, i.e., incremental effectiveness (IE), to identify treatment-related changes. In contrast, model 2 reflects the effectiveness of FET PET alone to differentiate tumor relapse from treatment-related changes. This different calculation method is in line with a previous study that assessed the cost-effectiveness of FET PET for the same indication in patients with brain metastases [32].

Model 1 (Fig. 2): Pretreated CNS lesions underwent both [18F]FET PET and MRI to differentiate between tumor relapse and treatment-related changes. Chance nodes one and two divided lesions into groups, depending on the combined [18F]FET PET and MRI findings (N1) or MRI findings alone (N2) (i.e., tumor relapse and treatment-related changes), respectively. The subsequent chance nodes N3-6 assigned each of these four groups of lesions rated as tumor relapse or treatment-related changes to their confirmed diagnosis.

Model 2 (Fig. 2): In pretreated CNS lesions with routine MRI findings suspicious for tumor relapse, [<sup>18</sup>F]FET PET was additionally performed to differentiate between tumor relapse and treatment-related changes. Chance node one (N1) divided lesions into groups depending on individual [<sup>18</sup>F]FET PET findings (tumor relapse and treatment-related changes). The subsequent chance nodes N2-3 assigned each

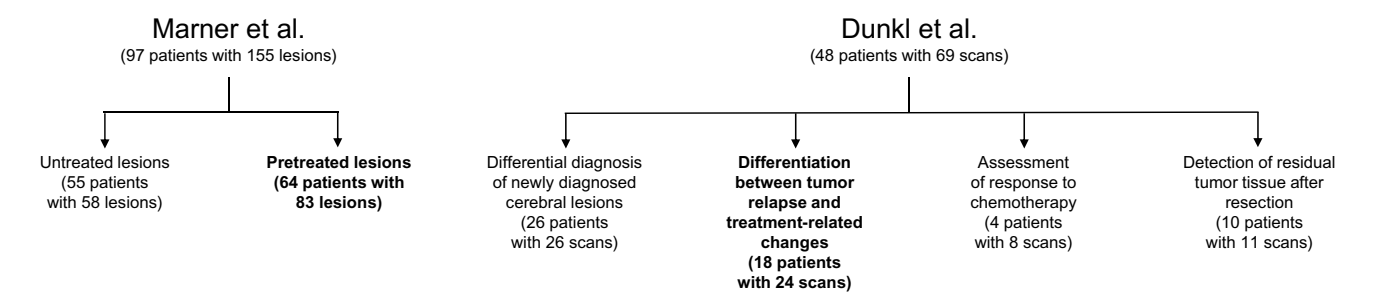
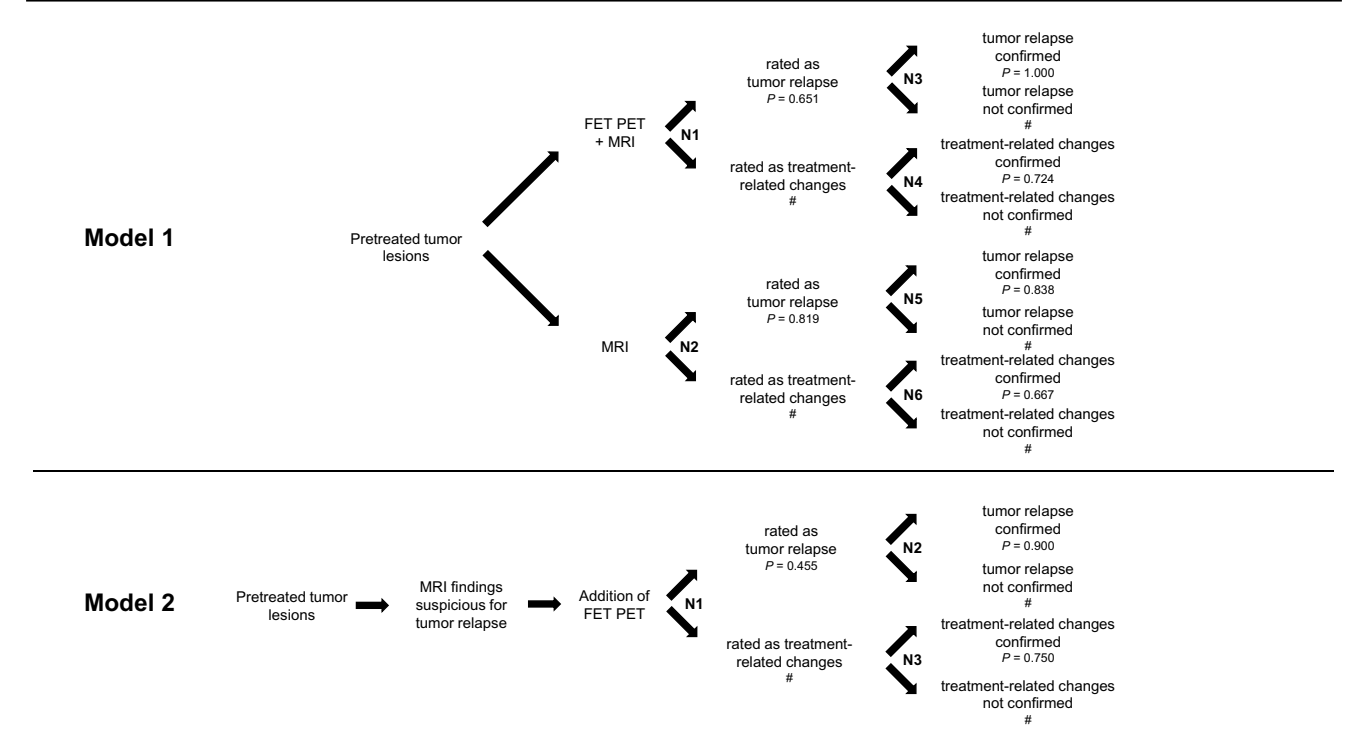


Fig. 1 Patient selection for the cost-effectiveness analysis (in bold) from the studies of Marner et al. [23] and Dunkl et al. [19]. Note that due to exclusions and serial scanning during follow-up the numbers do not further increase





**Fig. 2** Model 1 (upper panel): Decision tree model for assessment of the effectiveness of additional [<sup>18</sup>F]FET PET to differentiate between tumor relapse and treatment-related changes (n=83). The model includes the two alternative strategies of using MRI alone or in combination with [<sup>18</sup>F]FET PET. Chance nodes N1 and N2 divide lesions in tumor relapse or treatment-related changes based on [<sup>18</sup>F] FET PET combined with MRI or MRI alone. Subsequent nodes N3-N6 assigned lesions with tumor relapse or treatment-related changes to their confirmed diagnosis based on neuropathological findings or the clinicoradiological follow-up. *P*-values indicate the probability that a lesion is rated as tumor relapse (N1-2) or that the respective imaging diagnosis is confirmed (N3-6). Abbreviations: #=corresponding likeli-

of these two groups of lesions rated as tumor relapse or treatment-related changes to their confirmed diagnosis.

For both decision trees, we defined the probability of the correct identification of treatment-related changes as the primary outcome.

#### **Cost calculation**

The costs were calculated from the perspective of the German Statutory Health Insurance system. As the German statutory health insurance companies has thus far not covered [18F]FET PET costs in the care of children or adolescents with CNS tumors, the costs for both [18F]FET PET and conventional MR imaging were calculated based on the "Medical Fee Schedule for Care Outside the Statutory Health Insurance Scheme" (http://www.e-bis.de/goae/defau ltFrame.htm) to provide an equal and consistent determination of the cost.

As described previously [29], the costs taken into consideration for [18F]FET PET were as follows (procedure's

hood (1-*P*); N1-6=chance nodes 1–6. Model 2 (lower panel): Decision tree for assessment of the effectiveness of additional [<sup>18</sup>F]FET PET to diagnose treatment-related changes (n=22) when routine MRI findings were suspicious for tumor relapse. Chance node N1 divides lesions into tumor relapse and treatment-related changes according to [.<sup>18</sup>F]FET PET findings. Subsequent nodes N2-3 assign lesions rated as tumor relapse or treatment-related changes to their confirmed diagnosis based on neuropathological findings or the clinicoradiological follow-up. *P*-values indicate the probability that a lesion is rated as tumor relapse (N1) or that the imaging diagnosis is confirmed (N2-3). Abbreviations: #=corresponding likelihood (1-*P*); N1-3=chance nodes 1–3

index number in parenthesis): Patient consultation €10.72 (1), report on diagnostic findings €17.43 (75), intravenous injection €9.38 (253), scintigraphy of the brain €125.91 (5430), [<sup>18</sup>F]FET PET with quantitative analysis €786.89 (5489), and tracer production costs of €616.00. For MRI, the expenses were as follows: Patient consultation €10.72 (1), physical examination €10.72 (5), report on diagnostic findings €17.43 (75), high-pressure intravenous injection €40.23 (346), surcharge for perfusion imaging €75.19 (3051), MRI with three-dimensional and apparent diffusion coefficient (ADC) reconstruction requiring substantial technical effort €641.16 (5700), additional MRI series with three-dimensional and ADC reconstruction requiring substantial technical effort €145.72 (5731), and surcharge for computer analysis €46.63 (5733). Thus, the imaging costs for one [18F]FET PET were estimated at €1,566.33 and €987.80 for one MRI scan.

In decision tree model 1, the identification of a lesion consistent with treatment-related changes comprised one [18F]FET PET and one MRI scan. Thus, the costs of both



imaging modalities were added for cost calculation. Moreover, as 92 scans were performed for 83 treated lesions, an additional factor (i.e., 92/83) for the cost calculation was considered, resulting in imaging costs of  $\epsilon$ 2,831.08 per lesion. In decision tree model 2, the identification of a lesion consistent with treatment-related changes comprised one [ $^{18}$ F]FET PET scan. Therefore, the imaging costs per lesion resulted in  $\epsilon$ 1,566.33.

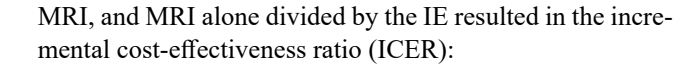
#### **Cost-effectiveness**

In decision tree model 1, the effectiveness of the correct identification of treatment-related changes was compared between the combined [18F]FET PET and MRI approach, and MRI alone (i.e., incremental effectiveness (IE)). Hence, the difference in cost between [18F]FET PET combined with

**Table 1** Chance node intervals and corresponding effectiveness and CER in the one-way deterministic sensitivity analysis for decision tree models 1 and 2

| Chance<br>node | Parameter         | Decision tree model |                   | Decision tree<br>model 2 |                   |
|----------------|-------------------|---------------------|-------------------|--------------------------|-------------------|
|                |                   | lower<br>interval   | upper<br>interval | lower<br>interval        | upper<br>interval |
|                | Value (%)         | 50                  | 80                | 31                       | 61                |
| N1             | Effectiveness (%) | 52                  | 52                | 95                       | 83                |
|                | CER (€)           | 3,314.51            | 3,314.51          | 1,657.78                 | 1,885.60          |
|                | Value (%)         | 67                  | 97                | 83                       | 98                |
| N2             | Effectiveness (%) | 33                  | 88                | 84                       | 97                |
|                | CER (€)           | 5,271.88            | 1,962.97          | 1,870.89                 | 1,609.84          |
|                | Value (%)         | 93                  | 108*              | 68                       | 83                |
| N3             | Effectiveness (%) | 36                  | 76*               | 89                       | 91                |
|                | CER (€)           | 4,794.30            | 2,276.21*         | 1,759.70                 | 1,724.55          |
|                | Value (%)         | 65                  | 80                |                          |                   |
| N4             | Effectiveness (%) | 52                  | 52                | n.a                      | n.a               |
|                | CER (€)           | 3,314.51            | 3,314.51          |                          |                   |
|                | Value (%)         | 76                  | 91                |                          |                   |
| N5             | Effectiveness (%) | 62                  | 37                | n.a                      | n.a               |
|                | CER (€)           | 2,814.54            | 4,678.84          |                          |                   |
|                | Value (%)         | 59                  | 74                |                          |                   |
| N6             | Effectiveness (%) | 55                  | 50                | n.a                      | n.a               |
|                | CER (€)           | 3,136.95            | 3,492.08          |                          |                   |

The effectiveness and the cost-effectiveness ratio were calculated based on the indicated change node values. Note that (i) values for the effectiveness and the cost-effectiveness ratio of decision tree model 1 correspond to incremental values (difference between [<sup>18</sup>F]FET PET+MRI and MRI alone), and (ii) decision tree model 2 comprises only chance nodes N1-3. Abbreviations: *CER* cost-effectiveness ratio; *n.a.* not applicable



In decision tree model 2, the effectiveness of correct identification of treatment-related changes was calculated for [<sup>18</sup>F] FET PET alone. Thus, the cost for one FET PET divided by its effectiveness resulted in the cost-effectiveness ratio (CER):

$$CER = \frac{Cost ([18F]FET PET)}{Effectiveness ([18F]FET PET)}$$

# **Sensitivity analyses**

Deterministic and probabilistic sensitivity analyses were performed to test the robustness of the calculated effectiveness. In particular, one-way deterministic sensitivity analysis evaluated the impact of each independent variable (model 1, chance nodes N1-6; model 2, chance nodes N1-3) on the resulting effectiveness and, thus, the (incremental) cost-effectiveness ratio. Due to a lack of previous studies evaluating the cost-effectiveness of [18F]FET PET in children and adolescents with CNS tumors, and since the majority of analyzed lesions were gliomas, available confidence intervals already used in comparable studies that evaluated the cost-effectiveness of [18F]FET PET for treatment monitoring in adult patients with gliomas were applied to each variable (Table 1) [28–30]. In model 1, as the calculated value for N3 was 100%, changing that chance node value within the deterministic sensitivity analysis resulted in theoretical values > 100%. Thus, the resulting IE and ICER based on these values are likewise considered theoretical.

For probabilistic sensitivity analysis, a Monte Carlo analysis was performed using 10,000 sets of positive random values for the independent variables (Model 1, chance nodes N1-6; Model 2, chance nodes N1-3). The distribution of these random values was defined by the mean of the decision trees and the standard deviation, which was set according to the respective confidence interval of the deterministic sensitivity analysis, similar to earlier studies [28, 29] (Table 2). As described previously [29], for each set of random values, we determined the effectiveness separately for both [18F]FET PET and MRI, and their respective difference (i.e., IE) (Model 1), or the effectiveness of [18F]FET PET alone (Model 2). The (incremental) cost-effectiveness ratio was determined based on the effectiveness values.

Furthermore, imaging costs were modeled by a gamma distribution with the mean imaging cost per lesion and a



<sup>\*</sup>theoretical values as N3>100%

Table 2 Values for decision tree models 1 and 2 and Monte Carlo analysis

| Chance node | Decision tre | e model 1 | Decision tre | Decision tree model 2 |  |
|-------------|--------------|-----------|--------------|-----------------------|--|
|             | Value (%)    | SD (%)    | Value (%)    | SD (%)                |  |
| N1          | 65           | 8         | 46           | 8                     |  |
| N2          | 82           | 8         | 90           | 4                     |  |
| N3          | 100          | 4         | 75           | 4                     |  |
| N4          | 72           | 4         | n.a          | n.a                   |  |
| N5          | 84           | 4         | n.a          | n.a                   |  |
| N6          | 67           | 4         | n.a          | n.a                   |  |

The values for the chance nodes were calculated based on the data by Marner et al. (Model 1) and Dunkl et al. (Model 2). Standard deviations were set according to the confidence intervals of the deterministic sensitivity analysis, as reported previously [28, 29]. Note that decision tree model 2 comprises only chance nodes N1-3. Abbreviations: *SD* standard deviation; *n.a.* not applicable

standard deviation of 50% of the corresponding mean. The probabilistic sensitivity analysis results for effectiveness values were displayed by mean, median, standard deviation, 95% confidence interval (CI), minimum and maximum values, and the 2.5 th-, 10 th-, 90 th-, 97.5 th-percentiles. All calculations, Figures, and simulations were performed using the statistical computing language and environment software R [33–35].

# Results

# **Effectiveness**

Decision tree model 1 revealed that adding [<sup>18</sup>F]FET PET to MRI increased the fraction of correctly identified treatment-related changes by 52% (correct identification by [<sup>18</sup>F]FET PET and MRI vs. MRI alone, 100% vs. 48%). Thus, two lesions had to be examined to identify one additional lesion consistent with treatment-related changes using [<sup>18</sup>F]FET PET. Decision tree model 2 revealed that [<sup>18</sup>F]FET PET correctly identified treatment-related changes in 90% of lesions when routine MRI findings were suspicious for tumor relapse. Thus, two lesions had to be examined to identify one lesion consistent with treatment-related changes by [<sup>18</sup>F]FET PET. Calculated values for the chance nodes of both decision trees are indicated in Fig. 2 and Table 2.

# **Cost-effectiveness**

For decision tree model 1, the ICER, i.e., the cost to correctly identify one additional lesion consistent with treatment-related changes by adding [<sup>18</sup>F]FET PET to MRI that would have been misclassified using MRI alone, resulted in €3,314.51. For decision tree model 2, the CER, i.e., the cost of correctly identifying one additional lesion consistent with

treatment-related changes when routine MRI findings were suspicious for tumor relapse, resulted in €1,740.37.

# Sensitivity analyses

For decision tree model 1, the resulting IE and ICER for the chance node intervals of the deterministic sensitivity analysis are presented in Table 1. The upper panel in Fig. 3 shows the corresponding Tornado diagram. The range of ICER values was  $\[mathebox{\in} 1,962.97\]$ — $\[mathebox{\in} 5,271.88$ . The results for both the IE and ICER of the probabilistic sensitivity analysis exceeded the calculated values of the decision tree (mean IE, 55%; 95% CI, 58—68%; mean ICER,  $\[mathebox{\in} 3,146.05; 95\%\]$  CI,  $\[mathebox{\in} 2,545.75\]$ — $\[mathebox{\in} 3,009.63$ ) (Table 3; upper panel in Fig. 4).

For decision tree model 2, the resulting effectiveness and CER for the chance node intervals of the deterministic sensitivity analysis are presented in Table 1. The lower panel in Fig. 3 shows the corresponding Tornado diagram. The range of CER values was €1,609.84—€1,885.60. The results of the probabilistic sensitivity analysis showed both a narrow distribution around the mean and a close relation to the calculated effectiveness and CER values of the decision tree (mean effectiveness, 90%; 95% CI, 80–97%; mean CER, €1,743.94; 95% CI, €1,608.53—€1,968.27) (Table 3; lower panel in Fig. 4). This close relation confirmed the robustness and reliability of the calculated values of the decision tree.

# **Discussion**

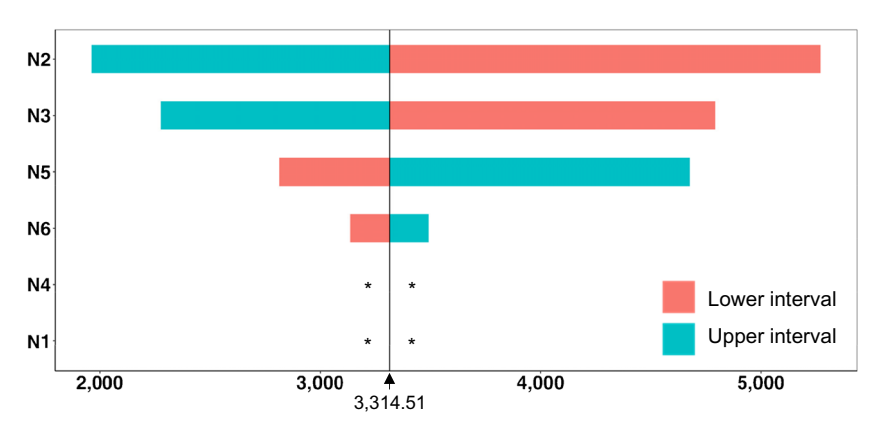
The main finding of the present study is that [18F]FET PET was cost-effective in identifying treatment-related changes in children and adolescents with pretreated CNS tumors.

The robustness of the results was supported by the comparatively small range of the deterministic and probabilistic sensitivity analysis results. Besides, for decision tree 1, the results of the probabilistic sensitivity analysis suggested even higher values for the IE, with a more favorable mean of 55% and a 95% CI of 58–68%, which exceeded the calculated value of the decision tree (i.e., 52%). The fact that the calculated values were outside the indicated CI may raise questions regarding the robustness of the results. Nevertheless, this deviation was merely a result of the calculation method of probabilistic sensitivity analysis. In any case, these results reflected the diagnostic value of [<sup>18</sup>F]FET PET for identifying treatment-related changes in this patient group.

The clinical scenarios illustrated in the decision tree models 1 and 2 showed differences in the analyzed patient groups regarding tumor types, pretreatment, and the temporal sequence of neuroimaging. In both scenarios, our results were based on identifying treatment-related changes since



Fig. 3 Tornado diagrams of the (incremental) cost-effectiveness ratio of [<sup>18</sup>F]FET PET for the identification of treatment-related changes (Model 1, upper panel), and treatment-related changes when routine MRI findings were suspicious for tumor relapse (Model 2, lower panel). The indicated (incremental) cost-effectiveness ratios resulted from applying the upper and lower interval values of the one-way deterministic sensitivity analysis onto change nodes N1-6 and N1-3, respectively. \*Applying interval values on N4 and N1 did not affect the resulting incremental cost-effectiveness ratios



Incremental cost-effectiveness ratio of FET PET (€)

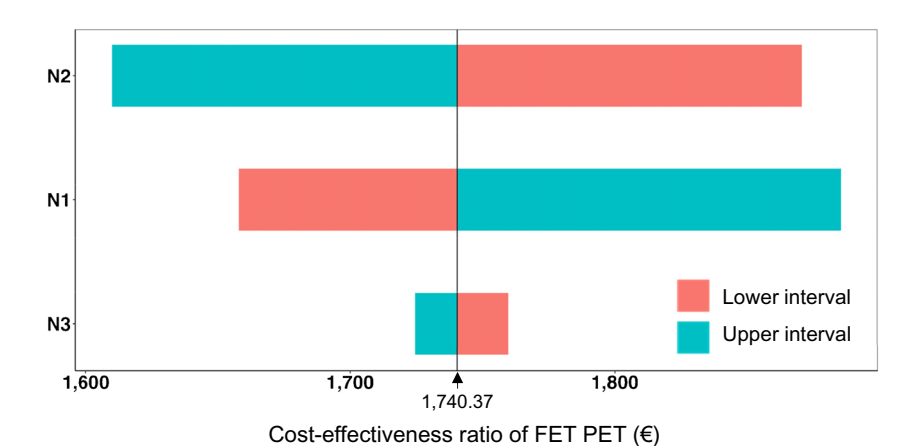


Table 3 Statistics resulting from the Monte Carlo analysis, including 10,000 samples for the effectiveness

| Value/<br>Percentile | Decision tree model 1 |                                    |        |   | Decision tree model 2         |   |
|----------------------|-----------------------|------------------------------------|--------|---|-------------------------------|---|
|                      | MRI (%)               | [ <sup>18</sup> F]FET PET +MRI (%) | IE (%) | Cost for<br>additional<br>[ <sup>18</sup> F]FET PET (€) | [ <sup>18</sup> F]FET PET (%) | Cost for<br>additional<br>[ <sup>18</sup> F]FET PET (€) |
| Mean                 | 46                    | 101*                               | 55*    | 1,719.62  | 90                            | 1,551.39  |
| SD                   | 15                    | 13                                 |        | 862.13  | 5                             | 777.79  |
| Minimum              | -91*                  | 59                                 | 150*   | 98.65   | 66                            | 89.00   |
| 2.5 th               | 13                    | 81                                 | 68     | 488,74  | 80                            | 440.92  |
| 10 th                | 27                    | 89                                 | 62     | 759.79  | 84                            | 685.46  |
| Median               | 48                    | 100                                | 52     | 1,573.98  | 90                            | 1,420.00  |
| 90 th                | 64                    | 115*                               | 51*    | 2,865.63  | 95                            | 2,585.29  |
| 97.5 th              | 71                    | 129*                               | 58*    | 3,814.70  | 97                            | 3,441.53  |
| Maximum              | 96                    | 430*                               | 335*   | 7.222.32  | 104*                          | 6,515.79  |

Columns indicate the probability of correct identification of treatment-related changes (Model 1), and treatment-related changes when routine MRI findings were suspicious for tumor relapse (Model 2) by the indicated imaging modality. Column IE indicates the difference of probabilities and thus the incremental effectiveness in using [18F]FET PET. Column Cost for additional [18F]FET PET indicates the gamma-distributed additional [18F]FET PET imaging cost per lesion. Abbreviations: *IE* incremental effectiveness; *SD* standard deviation

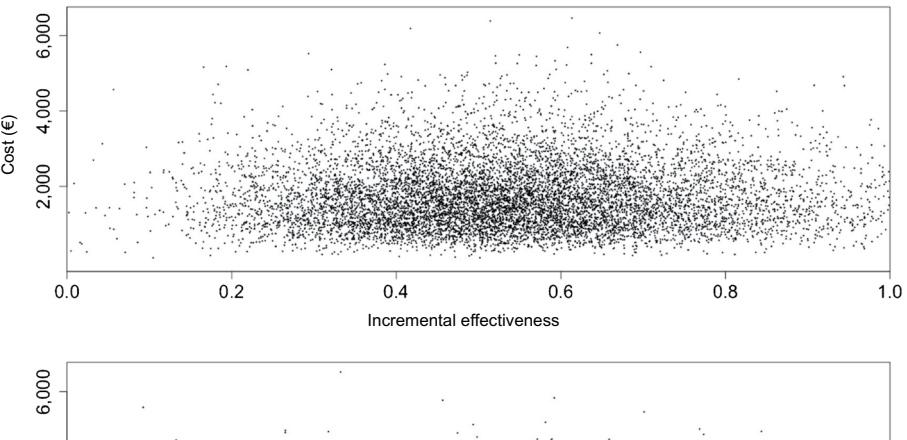
this identification considerably influences further treatment planning in affected patients. This particularly applied to clinical situations in which treatment-related changes such as pseudoprogression on MRI may lead to a discontinuation of a potentially effective treatment based on the false assumption of tumor relapse. Thus, a premature and more aggressive treatment regimen, including surgical interventions, with the risk of severe side effects and a decrease in health-related quality of life, can be avoided.

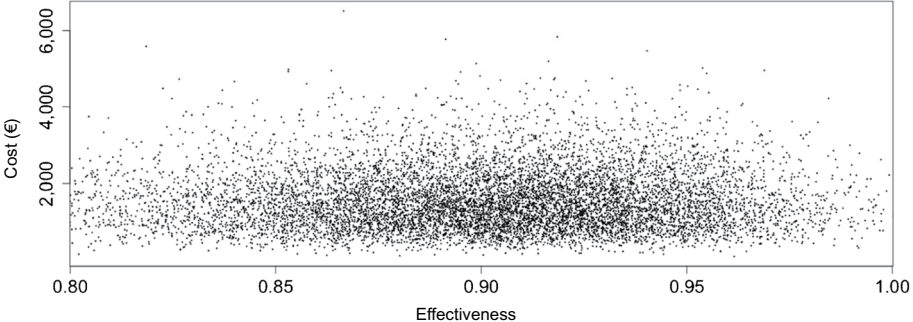
From an economic point of view, the exact amount of potentially saved cost due to an avoidance of a probably more costly and more aggressive treatment option by



<sup>\*</sup> theoretical values

Fig. 4 Distribution of results from Monte Carlo analysis (dots) about the effectiveness of [<sup>18</sup>F]FET PET for the identification of treatment-related changes (Model 1, upper panel) and treatment-related changes when routine MRI findings were suspicious for tumor relapse (Model 2, lower panel). Note that the x-axes of the panels are differently scaled. Margin values are not shown





adding [<sup>18</sup>F]FET PET to the diagnostic work-up was almost impossible to assess given the number of available treatment options for various CNS tumor types in the evaluated groups of pediatric and adolescent patients. For glioblastomas, the overall cost of standard treatment consisting of radiotherapy with concomitant and six cycles of adjuvant temozolomide chemotherapy is approximately €30,000 [36, 37], the comparatively lower expense for [<sup>18</sup>F]FET PET for differentiating between tumor relapse and treatment-related changes seems to be cost-effective.

In comparison to other studies evaluating the cost-effectiveness of [18F]FET PET for assessment of tumor lesions in adult patients with gliomas compared to MRI, the calculated ICER of decision tree 1 was lower and thus more favorable, confirming the cost-effectiveness of [18F]FET PET for the identification of treatment-related changes in this patient group [27, 29, 30]. Similarly, compared to two other studies that investigated the cost-effectiveness of [<sup>18</sup>F] FET PET for evaluating brain metastasis relapse following radiotherapy alone or multimodal therapy, including radiotherapy, targeted therapy, checkpoint inhibitors, and combinations thereof, the calculated ICER of decision tree 1 was lower [31, 32]. Only one study that investigated the cost-effectiveness of [18F]FET PET for assessing treatment response in patients with gliomas showed lower results for the ICER [28]. This difference was likely due to differences in the cost calculation that was done in the context of Belgian healthcare system in the mentioned study, while the underlying results for the IE were similar to the present results [28]. In principle, comparability of the results was limited as the studies above exclusively investigated the cost-effectiveness of [<sup>18</sup>F]FET PET in the care of adult patients, and the assessed clinical scenarios differed from the scenarios assessed in the present study.

Other advanced imaging modalities, such as diffusion- or perfusion-weighted MR imaging, and proton magnetic resonance spectroscopy can similarly contribute further details on the underlying biology of tumors, particularly regarding molecular, physiological, and functional characteristics [38]. With regard to perfusion MRI, its diagnostic accuracy appears to be inferior compared to FET PET for differentiating tumor relapse and treatment-related changes in adult patients [39]. Moreover, advanced MR imaging remains relatively non-standardized, as outputs are considerably influenced by scanner-specific parameters, particularly the choice and configuration of sequences [40]. In contrast, FET PET acquisition has been standardized [41], allowing for more consistent and comparable results across different institutions. Furthermore, the value of advanced MRI techniques was predominantly assessed in adult patients, and data obtained in pediatric patients with brain tumors remain still scarce.

There are a number of limitations of the present study that warrant further consideration. First, although the majority of the assessed tumor lesions were gliomas, the tumors evaluated in our study are to a certain degree heterogenous in terms of neuropathological diagnosis and location, such as spinal lesions. Nevertheless, we did not exclude these lesions from the analysis since diagnostic and therapeutic interventions are widely comparable. In particular, the value of additional FET PET for identifying treatment-related changes has been demonstrated for all types of lesions in



the studies on which our analysis is based. Secondary brain tumors were not included. Second, a putative limitation of the present results for the cost-effectiveness ratios was their focus on individual lesions. This aspect needs to be considered in patients with multiple lesions as these result in repetitive scans and consequently higher expenses. Notwithstanding, by focusing on the individual lesion, the present results are more generalizable to other patients as the number of lesions naturalistically varies between patients. In addition, we considered the number of scans for each individual lesion to realistically reflect increased cost for serial scanning. The third limitation was that the cost calculation was conducted within the context of a specific, i.e., German healthcare system, using a similar approach to evaluate (cost-) effectiveness of [18F]FET PET for other indications in patients with brain tumors as described earlier [26-31]. Consequently, the present results for the (incremental) cost-effectiveness ratios could not directly be transfered to other countries due to national differences in healthcare and cost structures. For example, in Belgium, cost for [18F]FET PET scanning are considerably lower (cost for one [18F]FET PET approximately €400) due to national grants, distinct reimbursement schemes, and dependency of cost from the number of annually performed [18F]FET PET scans [28]. Of note, if the Belgian scanning cost were taken as a basis for the present analysis, the resulting costeffectiveness of [18F]FET PET would probably have been even more favorable [28]. In addition, the present results for the (incremental) effectiveness (i.e., the probability of correctly identifying treatment-related changes) appeared to be transferable to other countries as these predominantly depended on the information obtained from the respective neuroimaging modality. Thus, the present data showing an (incremental) effectiveness may help physicians choose the most appropriate neuroimaging approach during follow-up and considerably facilitate further cost evaluations from the perspective of health economics.

# **Conclusion**

This study suggests that [<sup>18</sup>F]FET PET is cost-effective for identification of treatment-related changes in pretreated CNS tumors in children and adolescents and improves patient care at acceptable costs.

**Supplementary Information** The online version contains supplementary material available at https://doi.org/10.1007/s00259-025-07377-x.

Author contributions Study design: Norbert Galldiks, Jurij Rosen, Karl-Josef Langen.

Data acquisition: Jurij Rosen, Jan-Michael Werner, Garry S. Ceccon, Elena K. Rosen, Michael M. Wollring, Isabelle Stetter, Lisbeth Marn-

er, Ian Law, Norbert Galldiks.

Data analysis, writing of manuscript drafts: Jurij Rosen, Elena K. Rosen, Norbert Galldiks.

Interpretation of data: Jurij Rosen, Philipp Lohmann, Felix M. Mottaghy, Lisbeth Marner, Ian Law, Gereon R. Fink, Karl-Josef Langen, Norbert Galldiks.

Revising manuscript, approving final content of manuscript: all.

Funding Open Access funding enabled and organized by Projekt DEAL.

None.

**Data availability** The datasets generated during and/or analyzed during the current study are available from the corresponding author on reasonable request.

#### **Declarations**

**Ethics approval** The input data of the present study were derived from the results of previously published studies by Marner et al. [23] and Dunkl et al. [19]. These studies had been performed in line with the principles of the Declaration of Helsinki and the respective institutional review board had approved these studies (Marner et al., file number: H-6–2014-095; Dunkl et al., file number: EK 022/14).

**Consent to participate** Informed consent had been obtained from the legal guardians of the minor study participants included in the study.

**Consent to publish** The legal guardians of the minor study participants had given written informed consent for assessment of clinical data for scientific purposes and subsequent publication.

Competing interests NG received honoraria for lectures from Blue Earth Diagnostics, for advisory board participation from Telix Pharmaceuticals and Servier, and for consultancy services from Telix Pharmaceuticals. PL received honoraria for lectures from Blue Earth Diagnostics. KL received honoraria from Telix Pharmaceuticals for consultancy services. FMM is an Editor of the European Journal of Nuclear Medicine and Molecular Imaging. The other authors disclosed no potential conflicts of interest related to the present work.

**Open Access** This article is licensed under a Creative Commons Attribution 4.0 International License, which permits use, sharing, adaptation, distribution and reproduction in any medium or format, as long as you give appropriate credit to the original author(s) and the source, provide a link to the Creative Commons licence, and indicate if changes were made. The images or other third party material in this article are included in the article's Creative Commons licence, unless indicated otherwise in a credit line to the material. If material is not included in the article's Creative Commons licence and your intended use is not permitted by statutory regulation or exceeds the permitted use, you will need to obtain permission directly from the copyright holder. To view a copy of this licence, visit <a href="http://creativecommons.org/licenses/by/4.0/">http://creativecommons.org/licenses/by/4.0/</a>.

#### References

 Ostrom QT, Price M, Neff C, Cioffi G, Waite KA, Kruchko C, et al. CBTRUS statistical report: primary brain and other central nervous system tumors diagnosed in the United States in 2016– 2020. Neuro Oncol. 2023;25:iv1–99. https://doi.org/10.1093/neu onc/noad149.



- Piccardo A, Albert NL, Borgwardt L, Fahey FH, Hargrave D, Galldiks N, et al. Joint EANM/SIOPE/RAPNO practice guidelines/SNMMI procedure standards for imaging of paediatric gliomas using PET with radiolabelled amino acids and [(18)F]FDG: version 1.0. Eur J Nucl Med Mol Imaging. 2022;49:3852–69. htt ps://doi.org/10.1007/s00259-022-05817-6.
- Paugh BS, Qu C, Jones C, Liu Z, Adamowicz-Brice M, Zhang J, et al. Integrated molecular genetic profiling of pediatric high-grade gliomas reveals key differences with the adult disease. J Clin Oncol. 2010;28:3061–8. https://doi.org/10.1200/JCO.2009. 26.7252.
- Ryall S, Tabori U, Hawkins C. Pediatric low-grade glioma in the era of molecular diagnostics. Acta Neuropathol Commun. 2020;8:30. https://doi.org/10.1186/s40478-020-00902-z.
- Lohmann P, Stavrinou P, Lipke K, Bauer EK, Ceccon G, Werner JM, et al. FET PET reveals considerable spatial differences in tumour burden compared to conventional MRI in newly diagnosed glioblastoma. Eur J Nucl Med Mol Imaging. 2019;46:591–602. https://doi.org/10.1007/s00259-018-4188-8.
- Dhermain FG, Hau P, Lanfermann H, Jacobs AH, van den Bent MJ. Advanced MRI and PET imaging for assessment of treatment response in patients with gliomas. Lancet Neurol. 2010;9:906–20. https://doi.org/10.1016/S1474-4422(10)70181-2.
- Brandsma D, Stalpers L, Taal W, Sminia P, van den Bent MJ. Clinical features, mechanisms, and management of pseudoprogression in malignant gliomas. Lancet Oncol. 2008;9:453–61.
- da Cruz HLC Jr, Rodriguez I, Domingues RC, Gasparetto EL, Sorensen AG. Pseudoprogression and pseudoresponse: imaging challenges in the assessment of posttreatment glioma. AJNR Am J Neuroradiol. 2011;32:1978-85.
- Yang I, Aghi MK. New advances that enable identification of glioblastoma recurrence. Nat Rev Clin Oncol. 2009;6:648–57.
- Kumar AJ, Leeds NE, Fuller GN, Van Tassel P, Maor MH, Sawaya RE, et al. Malignant gliomas: MR imaging spectrum of radiation therapy- and chemotherapy-induced necrosis of the brain after treatment. Radiology. 2000;217:377–84. https://doi.org/10.1148/radiology.217.2.r00nv36377.
- 11. Langen KJ, Galldiks N, Hattingen E, Shah NJ. Advances in neuro-oncology imaging. Nat Rev Neurol. 2017;13:279–89. https://doi.org/10.1038/nrneurol.2017.44.
- Rapp M, Heinzel A, Galldiks N, Stoffels G, Felsberg J, Ewelt C, et al. Diagnostic performance of 18F-FET PET in newly diagnosed cerebral lesions suggestive of glioma. J Nucl Med. 2013;54:229–35.
- Suchorska B, Jansen NL, Linn J, Kretzschmar H, Janssen H, Eigenbrod S, et al. Biological tumor volume in 18FET-PET before radiochemotherapy correlates with survival in GBM. Neurology. 2015;84:710–9. https://doi.org/10.1212/WNL.000000000 0001262.
- Galldiks N, Dunkl V, Stoffels G, Hutterer M, Rapp M, Sabel M, et al. Diagnosis of pseudoprogression in patients with glioblastoma using O-(2-[18F]fluoroethyl)-L-tyrosine PET. Eur J Nucl Med Mol Imaging. 2015;42:685–95.
- Galldiks N, Stoffels G, Filss C, Rapp M, Blau T, Tscherpel C, et al. The use of dynamic O-(2–18F-fluoroethyl)-l-tyrosine PET in the diagnosis of patients with progressive and recurrent glioma. Neuro Oncol. 2015;17:1293–300. https://doi.org/10.1093/neuonc/nov088.
- Bashir A, Mathilde Jacobsen S, Molby Henriksen O, Broholm H, Urup T, Grunnet K, et al. Recurrent glioblastoma versus late posttreatment changes: diagnostic accuracy of O-(2-[18F] fluoroethyl)-L-tyrosine positron emission tomography (18F-FET PET). Neuro Oncol. 2019;21:1595–606. https://doi.org/10.1093/neuonc/noz166.
- 17. Werner JM, Stoffels G, Lichtenstein T, Borggrefe J, Lohmann P, Ceccon G, et al. Differentiation of treatment-related changes from

- tumour progression: a direct comparison between dynamic FET PET and ADC values obtained from DWI MRI. Eur J Nucl Med Mol Imaging. 2019;46:1889–901. https://doi.org/10.1007/s00259-019-04384-7.
- Werner JM, Weller J, Ceccon G, Schaub C, Tscherpel C, Lohmann P, et al. Diagnosis of pseudoprogression following lomustine-temozolomide chemoradiation in newly diagnosed glioblastoma patients using FET-PET. Clin Cancer Res. 2021;27:3704

  –13. https://doi.org/10.1158/1078-0432.CCR-21-0471.
- Dunkl V, Cleff C, Stoffels G, Judov N, Sarikaya-Seiwert S, Law I, et al. The usefulness of dynamic O-(2–18F-fluoroethyl)-L-tyrosine PET in the clinical evaluation of brain tumors in children and adolescents. J Nucl Med. 2015;56:88–92. https://doi.org/10.2967/jnumed.114.148734.
- Elahmadawy MA, El-Ayadi M, Ahmed S, Refaat A, Eltaoudy MH, Maher E, et al. F18-FET PET in pediatric brain tumors: integrative analysis of image derived parameters and clinico-pathological data. Q J Nucl Med Mol Imaging. 2023;67:46–56. https:// doi.org/10.23736/S1824-4785.20.03267-7.
- 21. Grosse F, Wedel F, Thomale UW, Steffen I, Koch A, Brenner W, et al. Benefit of static FET PET in pretreated pediatric brain tumor patients with equivocal conventional MRI results. Klin Padiatr. 2021;233:127–34. https://doi.org/10.1055/a-1335-4844.
- Kertels O, Krauss J, Monoranu CM, Samnick S, Dierks A, Kircher M, et al. [(18)F]FET-PET in children and adolescents with central nervous system tumors: does it support difficult clinical decision-making? Eur J Nucl Med Mol Imaging. 2023;50:1699–708. https://doi.org/10.1007/s00259-023-06114-6.
- Marner L, Lundemann M, Sehested A, Nysom K, Borgwardt L, Mathiasen R, et al. Diagnostic accuracy and clinical impact of [18F]FET PET in childhood CNS tumors. Neuro Oncol. 2021;23:2107–16. https://doi.org/10.1093/neuonc/noab096.
- Marner L, Nysom K, Sehested A, Borgwardt L, Mathiasen R, Henriksen OM, et al. Early postoperative (18)F-FET PET/MRI for pediatric brain and spinal cord tumors. J Nucl Med. 2019:60:1053–8. https://doi.org/10.2967/jnumed.118.220293.
- Misch M, Guggemos A, Driever PH, Koch A, Grosse F, Steffen IG, et al. (18)F-FET-PET guided surgical biopsy and resection in children and adolescence with brain tumors. Childs Nerv Syst. 2015;31:261–7. https://doi.org/10.1007/s00381-014-2552-y.
- Heinzel A, Stock S, Langen KJ, Muller D. Cost-effectiveness analysis of amino acid PET-guided surgery for supratentorial high-grade gliomas. J Nucl Med. 2012;53:552–8. https://doi.org/ 10.2967/jnumed.111.097352.
- Heinzel A, Stock S, Langen KJ, Muller D. Cost-effectiveness analysis of FET PET-guided target selection for the diagnosis of gliomas. Eur J Nucl Med Mol Imaging. 2012;39:1089–96. https://doi.org/10.1007/s00259-012-2093-0.
- Baguet T, Verhoeven J, De Vos F, Goethals I. Cost-effectiveness of [(18)F] fluoroethyl-L-tyrosine for temozolomide therapy assessment in patients with glioblastoma. Front Oncol. 2019;9:814. htt ps://doi.org/10.3389/fonc.2019.00814.
- Rosen J, Ceccon G, Bauer EK, Werner JM, Tscherpel C, Dunkl V, et al. Cost effectiveness of (18)F-FET PET for early treatment response assessment in glioma patients after adjuvant temozolomide chemotherapy. J Nucl Med. 2022;63:1677–82. https://doi.org/10.2967/jnumed.122.263790.
- Heinzel A, Muller D, Langen KJ, Blaum M, Verburg FA, Mottaghy FM, et al. The use of O-(2–18F-fluoroethyl)-L-tyrosine PET for treatment management of bevacizumab and irinotecan in patients with recurrent high-grade glioma: a cost-effectiveness analysis. J Nucl Med. 2013;54:1217–22. https://doi.org/10.2967/j numed.113.120089.
- 31. Heinzel A, Muller D, Yekta-Michael SS, Ceccon G, Langen KJ, Mottaghy FM, et al. O-(2–18F-fluoroethyl)-L-tyrosine PET for evaluation of brain metastasis recurrence after radiotherapy:



- an effectiveness and cost-effectiveness analysis. Neuro Oncol. 2017;19:1271–8. https://doi.org/10.1093/neuonc/now310.
- Rosen J, Werner JM, Ceccon GS, Rosen EK, Wollring MM, Stetter I, et al. MRI and (18)F-FET PET for Multimodal Treatment Monitoring in Patients with Brain Metastases: A Cost-Effectiveness Analysis. J Nucl Med. 2024;65:838–44. https://doi.org/10.2967/jnumed.123.266687.
- 33. R Core Team (2025) R: A Language and environment for statistical computing. R Foundation for Statistical Computing, Vienna, Austria. https://www.R-project.org/.
- 34. Wickham H, Averick M, Bryan J, Chang W, McGowan L, Francois R, et al. Welcome to the tidyverse. J Open Sour Softw. 2019;4(43):1686. https://doi.org/10.21105/joss.01686.
- 35. Wickham H, Bryan J (2023). readxl: Read Excel Files. https://readxl.tidyverse.org, https://github.com/tidyverse/readxl.
- 36. Uyl-de Groot CA, Stupp R, van der Bent M. Cost-effectiveness of temozolomide for the treatment of newly diagnosed glioblastoma multiforme. Expert Rev Pharmacoecon Outcomes Res. 2009;9:235–41. https://doi.org/10.1586/erp.09.15.
- Waschke A, Arefian H, Walter J, Hartmann M, Maschmann J, Kalff R. Cost-effectiveness of the long-term use of temozolomide for treating newly diagnosed glioblastoma in Germany. J Neurooncol. 2018;138:359–67. https://doi.org/10.1007/s11060-018-2 804-x.
- 38. Galldiks N, Kaufmann TJ, Vollmuth P, Lohmann P, Smits M, Veronesi MC, et al. Challenges, limitations, and pitfalls of PET

- and advanced MRI in patients with brain tumors: a report of the PET/RANO group. Neuro Oncol. 2024;26:1181–94. https://doi.org/10.1093/neuonc/noae049.
- Henriksen OM, Hansen AE, Muhic A, Marner L, Madsen K, Moller S, et al. Diagnostic yield of simultaneous dynamic contrast-enhanced magnetic resonance perfusion measurements and [(18)F]FET PET in patients with suspected recurrent anaplastic astrocytoma and glioblastoma. Eur J Nucl Med Mol Imaging. 2022;49:4677–91. https://doi.org/10.1007/s00259-022-05917-3.
- Patel P, Baradaran H, Delgado D, Askin G, Christos P, John Tsiouris A, et al. MR perfusion-weighted imaging in the evaluation of high-grade gliomas after treatment: a systematic review and meta-analysis. Neuro Oncol. 2017;19:118–27. https://doi.org/10.1093/neuonc/now148.
- 41. Law I, Albert NL, Arbizu J, Boellaard R, Drzezga A, Galldiks N, et al. Joint EANM/EANO/RANO practice guidelines/SNMMI procedure standards for imaging of gliomas using PET with radiolabelled amino acids and [(18)F]FDG: version 1.0. Eur J Nucl Med Mol Imaging. 2019;46:540–57. https://doi.org/10.1007/s00259-018-4207-9.

**Publisher's Note** Springer Nature remains neutral with regard to jurisdictional claims in published maps and institutional affiliations.

